

Numerical method for thixotropic behavior of fresh concrete

Zhuguo Li*, Guodong Cao, Kun Guo

Graduate School of Science and Technology for Innovation, Yamaguchi University, Ube, Yamaguchi, Japan



HIGHLIGHTS

- A rest & shearing time-dependent Discrete Element Method (DEM) was developed for the prediction of time-dependent fluidity of fresh concrete
- The effects of cement hydration, physical flocculation of cement particles and agitation was considered on the numerical analysis of time-dependent fluidity of fresh concrete.
- The changes of chemically bonded, flocculated, and dispersed particles in quantity with agitating time in agitated state, later after rest for a certain time, were clarified theoretically.
- The rest & shearing time-dependent DEM was confirmed to be applicable to the prediction of the change of fluidity in agitated state and the hysteresis loop for fresh concrete with or without addition of mineral admixture.

ARTICLE INFO

Article history:

Received 20 March 2018
Received in revised form 19 July 2018
Accepted 26 July 2018

Keywords:

Fresh concrete
Time-dependence
Physical flocculation
Cement hydration
Agitation
Discrete Element Method (DEM)
Hysteresis loop

ABSTRACT

The thixotropic characteristic or rest & shearing time-dependence of fluidity of fresh concrete has an influence on its production and construction processes. In this paper, the mechanisms of the thixotropy and rest & shearing time-dependence were discussed, followed by proposing an analytical approach to numerical prediction of the rest & agitating time-dependent flow behaviors on the basis of Discrete Element Method (DEM). In this new DEM, the effects of cement hydration, physical flocculation of cementitious particles, and agitation were taken into account. To validate the numerical method, the rheological tests of fresh mortars with or without mineral admixtures were performed after the mortar samples stood still for different times, using the B-type viscometer, of which the rotor's rotation would break down its surrounding particles' flocculation structure. The numerical results of torque-rotational speed relationship were close to the experimental results.

© 2018 Elsevier Ltd. All rights reserved.

1. Introduction

Fresh concrete is essentially a particle assembly containing water. From mixing to placement, the rheological properties change with the elapsed time. With the increase of rest time, the fluidity declines. However, re-mixing or agitation may recover partly the fluidity. This characteristic is usually called thixotropy or time-dependence. Hence, ready-mixed concrete usually needs to be mixed again in mixer or agitator truck before pumping or casting. The thixotropic behavior greatly influences the workability and the construction quality of concrete, such as flow ability decline during waiting to pump, slump loss even re-mixing in agitator truck before pumping, fluidity gain under a vibration in

mould, change of formwork pressure [1], collapse in 3D concrete printing [2], and weak concrete joint [3].

The fluidity decline of cementitious materials at rest is resulted from physical flocculation and hydration of cement particles [4]. The flocculated particles enclose the mixing water and the hydration consumes the mixing water so that free water is reduced. And the structural buildup would increase mean particle contact angle (θ_m) and mean inter-particle angle (ϕ_m) to raise the deformation resistance of fresh cementitious material [5]. The fluidity gain after re-mixed again is attributed to the breakdown of the flocculent structure, which releases the enclosed water, and the decrease of θ_m and ϕ_m .

The thixotropy is generally evaluated by the area of hysteresis loop formed by the up and down curves of torque and rotational speed relationship [6,7]. However, the hysteresis loop depends on loading history (e. g. re-mixing, agitating, and tamping before or while sample is filled into rheometer), growth rate of rotational

* Corresponding author.

E-mail address: li@yamaguchi-u.ac.jp (Z. Li).

speed, and maximum rotational speed, etc. [8]. It is believed that these factors affect the breakdown degree of the flocculent structure of particles. The thixotropy is also always described by the decrease of torque under a constant rotational speed or the increase of rotational speed under a constant torque with the elapsed time. However, if the rotational speed or the torque is kept to be a too small constant value, the corresponding torque increases, or the corresponding rotational speed decrease [8,9].

The physical flocculation and the hydration of cement particles generate the network of interactions between particles. The physically flocculated particles can be easily dispersed again by an agitation. However, the network structured by the hydrates is usually strong. The shear rejuvenation is mainly attributed to the destruction of flocculent structure of particles. Coussot et al. proposed a phenomenological model to predict shear stress–shear rate curve later after a rest time [9]. But it is only valid for short rest time [10]. Ignoring the effect of cement hydration is one of the reasons.

Roussel proposed another phenomenological model to describe the thixotropic behavior after a relatively long rest time [11]. Roussel found that the shear stress, corresponding to a certain shear rate, is a linear function of rest time. However, Lecompte and Perrot concluded that the relationship between yield stress and rest time becomes non-linear over longer time scale [4]. The yield stress is resulted from the microstructure of particles in fresh concrete [12]. The yield stress and apparent viscosity decrease when the microstructure is destroyed by shearing, but conversely increase when the microstructure reforms at rest. That is to say, the rheological properties of fresh concrete are rest & shearing time dependent. For properly evaluating fresh concrete's rheological properties and predicting its flow behavior, the rest & shearing time dependence or the thixotropy must be considered.

Discrete Element Method (DEM), as a particle approach, is well applied to the flow simulation of fresh concrete [13–16]. In general DEM, a parallel bond model is usually used to describe the interaction and re-dispersion condition of flocculated particles. The dispersion of the flocculated particles occurs only when their subjected forces are greater than the bond strength limits of particle–particle contact. The bond strength limits and the normal and shear stiffnesses of the parallel bond model are generally constants. However, for fresh cementitious materials, the particle contacts increase with time due to physical flocculation and cement hydration. Thus, for a given external force, its ability of destroying the inter-particle contacts or bonds decreases with time. In order to numerically analyze the rest time-dependence of fresh concrete's fluidity, the authors proposed a rest time-dependent DEM [13]. In this DEM, we introduced clumped particles with rigid contacts to reflect the effect of the hydrates, and let the normal and shear stiffnesses of the parallel bond model change with the number of flocculated particles, i.e. with rest time in consideration of the effects of physical flocculation and cement hydration. We further confirmed that the rest time-dependent DEM is also applied to the concrete that uses mineral admixtures in place of part of Portland cement, such as fly ash and ground granulated blast furnace slag [14].

In order to predict the thixotropic behavior, i.e. rest & shearing time-dependence of fresh concrete's fluidity, in this study we first investigated theoretically the particle dispersion under a shear force, and then expanded the rest time-dependent DEM to rest & shearing time-dependent DEM (td-DEM). By this td-DEM, not only the fluidity decline in standing state but also the rejuvenation under shear can be predicted numerically.

For verifying the td-DEM, we further did rheological tests of three kinds of fresh mortars, using a B-type viscometer to measure the torque-rotating speed relational curves after different rest times. It is considered that the rotation of viscometer's rotor would partly break down its surrounding inter-particle's structure.

Among the three mortar mixtures, two series of mortars used fly ash or ground granulated blast furnace slag in place of 20% or 50% of ordinary Portland cement. We also performed numerical analyses of the torque-rotational speed relationship by using the td-DEM, and compared them to the experimental results.

2. Proposal of DEM for thixotropy analysis of fresh concrete

2.1. Type of discrete particles and interaction

Two basic elements are used in present DEM: spherical (3D) particle and wall. The former is used to discretely express fresh concrete, and the latter is used to represent the boundary, such as sample container, mould, reinforced bar, and rheometer's blade. The particles move according to the Newton's Second Law, and the inter-particle force follows the force-displacement law. That is to say, the Newton's Second Law determines the motion of each particle subjected to inter-particle force, while the force-displacement law is used to calculate the inter-particle force arising from the relative motion at each contact point. The positions of wall elements are updated according to the wall motion velocity, unrelated to the Newton's Second Law.

Cement hydrates continually after it met water. The hydration products connect cementitious particles and aggregate particles. In standing state, because some of cementitious particles flocculate, the fluidity of fresh concrete goes down with rest time. However, if an agitation is applied to fresh concrete, the fluidity partially recovers because some of the flocculated particles are dispersed again. This is called thixotropy.

Therefore, three types of discrete particles should be considered for numerically analyzing the time-dependence of fluidity of fresh concrete by DEM: dispersed particles, chemically clumped particles, and physically flocculated particles.

In our past work [14], the interaction models were given for different types of discrete particle, as shown in Fig. 1. The interactions between two dispersed particles or dispersed particle and wall element are described by a viscous damping model, as shown in Fig. 1(a). The interactions consist of elastic force and viscous force that are expressed by springs with stiffnesses k_n^p and k_s^p , and dashpots with viscosity coefficients C_n and C_s , in normal and tangential directions, respectively. Slip is an intrinsic property and is described by a slip component.

The parallel bond model is used to express the interactions between two physically flocculated particles and their contact failure conditions, as shown in Fig. 1(b). The contact of flocculated particles is modeled as a set of springs with normal and shear stiffnesses k_n and k_s , uniformly distributed over a circular area on contact plane and centered at contact point. In general DEM, the stiffnesses k_n , k_s are dealt with two constants. But in present DEM, for describing the time-dependence of fresh concrete, the stiffnesses k_n , k_s should change with the number of flocculated particles. Besides k_n , k_s , the parallel bond model has other three parameters: normal and shear bond strength limit σ_c and τ_c , and bond-radius coefficient l . The σ_c and τ_c are used to describe the re-dispersion condition of flocculated particles. When the maximum tensile stress σ or shear stress τ acting on the contact point of two flocculated particles is greater than the σ_c or τ_c , the contact breaks and the two flocculated particles are accordingly dispersed again. Once flocculated particles are dispersed again by an agitation, their interactions follow the viscous damping model. The bond radius is a product of the bond-radius coefficient l and the minimum value of radius r_i , r_j of flocculated particle i and j [13].

On the other hand, the clumped particles in present DEM represent chemically bonded particles. They can't be dispersed again by an agitation or re-mixing. We described the contact of two

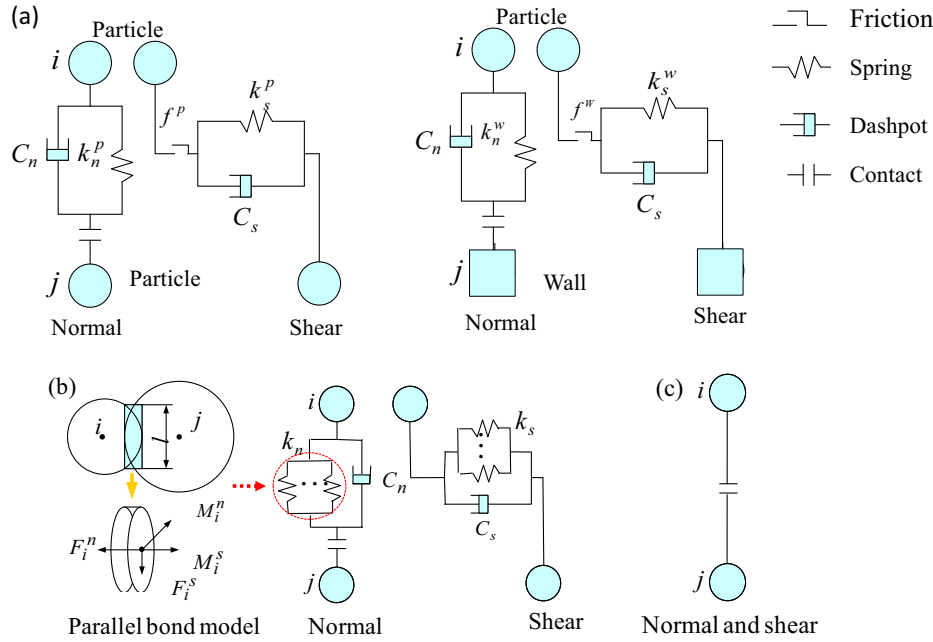


Fig. 1. Interaction model of DEM elements: (a) viscous damping model for two dispersed particles or particle and wall; (b) parallel bond model for two flocculated particles; (c) rigid bond model in clumped particle.

chemically clumped particles by a rigid bond model, as shown in Fig. 1(c). The mass of a clumped particle is equal to total mass of chemically bonded particles. The motion of particle is expressed in terms of the translational movement of its center and the rotation of the whole.

2.2. Numbers of various types of discrete particle

In our past work [14], we clarified the number (N_h) of the cementitious particles, which are bonded chemically by the hydrates, as shown in Eq. (1).

$$N_h = N \cdot \frac{t}{t_i} \cdot \exp\left[\frac{E}{R} \left(\frac{1}{293} - \frac{1}{273 + T}\right)\right] \quad (1)$$

where N is number of all cementitious particles, t is the elapsed time after mixing, t_i is initial setting time at 20 °C, E is activation energy of binder (J/mol), R is gas constant (8.3144 J/mol/K), and T is environmental temperature (°C)

The activation energy E is dependent on the specific surface area of binder, the chemical constituents of cement, the type and dosage of mineral admixture, and CaO content in fly ash, as shown in Eq. (2).

$$E = 22100 \cdot P_{C_3A}^{0.30} \cdot P_{C_4AF}^{0.25} \cdot B^{0.35} \cdot \left(1 - 1.05 \cdot P_{FA} \cdot \frac{P_{FA-CaO}}{0.40} + 0.40 \cdot P_{Slag}\right) \quad (2)$$

where $P_{C_3A}^{0.30}$, $P_{C_4AF}^{0.25}$ are contents of C_3A and C_4AF in cement by mass, respectively, B is specific surface area (m^2/kg) of binder, P_{FA} , P_{Slag} are replacing ratios of fly ash and ground granulated blast furnace slag by mass, and P_{FA-CaO} is CaO content in fly ash by mass

Also, we clarified the number (N_d) of the cementitious particles at time t , which are dispersed due to Brownian motion, as shown in Eq. (3) [14].

$$N_d = \frac{3\eta N_{d0}}{8kT N_{d0} + 3\eta} \quad (3)$$

where k is the Boltzmann constant, η is viscosity of mixing water, and N_{d0} is number of dispersed cementitious particles in the begin-

ning of standing state. If standing state starts right after fresh concrete was mixed, N_{d0} is equal approximately to N

Therefore, the number (N_f) of physically flocculated cementitious particles at a rest time point t_0 later after mixing can be expressed by Eq. (4) according to Eqs. (1) and (3).

$$N_f = N - (N_h)_{t=t_0} - (N_d)_{t=t_0} = N \cdot \left[1 - \beta \cdot t_0 - \frac{3\eta \cdot N_{d0}/N}{8kT \cdot N_{d0} \cdot t_0 + 3\eta}\right] \quad (4)$$

where is expressed by

$$\beta = \frac{1}{t_i} \cdot \exp\left[\frac{E}{R} \left(\frac{1}{293} - \frac{1}{273 + T}\right)\right] \quad (5)$$

As stated above, if an agitation or a shear force is applied to the fresh concrete that has been at a rest, some of physically flocculated cementitious particles will be dispersed again. In the following, the number of flocculated cementitious particles in agitated state is investigated by a theoretical analysis.

According to the author's past study [17], fresh concrete can be regarded as a viscous granular material, composed of cohesive particles (cementations particles), non-cohesive particles (aggregate particles), and water. The movement of cementitious particles is time-dependent, which causes a delayed deformation in fresh concrete, whereas aggregate particles instantaneously move when subjected to an inter-particle force. Hence, the shear deformation of fresh concrete is associated with the moving distances of all particles, but the shear strain rate of fresh concrete is only dependent on the movement rate of cementitious particles. The shear strain rate ($\dot{\gamma}$) of fresh concrete is equal to the product of the number (n) of moving cementitious particles occurring in unit time, the mean moving distance (A_{cm}) till they reach to each stable position, and the cosine value of mean particle contact angle of moving cementitious particles (θ_{cm}), as shown in Eq. (6).

$$\dot{\gamma} = \frac{dn}{dt^*} \cdot A_{cm} \cdot \cos\theta_{cm} \quad (6)$$

where t^* is lasting time of shear force, and A_{cm} , θ_{cm} are mean moving distance and mean particle contact angle of moving cementitious particles, respectively

Thus, the number of moving cementitious particles occurring in unit time in fresh concrete, i.e., the occurring rate (dn/dt) of moving cementitious particles, is expressed by Eq. (7)

$$\frac{dn}{dt^*} = \frac{1}{A_{cm} \cdot \cos\theta_{cm}} \cdot \dot{\gamma} \quad (7)$$

When a shear force acts on fresh concrete, some of flocculated particles are dispersed again and then move. It is considered that the more the flocculated cementitious particles and the greater the occurring rate (dn/dt) of moving cementitious particles, the more greatly the flocculated cementitious particles decrease in agitated state. In this study, we supposed that the decreasing rate of the flocculated cementitious particles is approximately proportional to the number (N_f) of flocculated cementitious particles at the time point of applying a shear force, and the occurring rate (dn/dt) of moving cementitious particles under the shear force, as shown in Eq. (8).

$$\frac{dN_f}{dt^*} \cong -\lambda \cdot N_f \cdot \frac{dn}{dt^*} \quad (8)$$

where λ is a proportional constant.

If substituting Eq. (7) into Eq. (8), Eq. (9) was obtained.

$$\frac{dN_f}{dt^*} \cong -\frac{\lambda \cdot \dot{\gamma}}{A_{cm} \cdot \cos\theta_{cm}} \cdot N_f \quad (9)$$

When agitating at a constant rotating speed, the shear strain rate ($\dot{\gamma}$) in Eq. (9) is constant. However, under agitation force control, the $\dot{\gamma}$ changes with shearing time even for a given shear force due to the breakdown of the flocculated structure of particles. Also, the mean cementitious particle contact angle (θ_{cm}) varies with the change of flocculated particles in quantity. For making Eq. (9) able to integrate, initial shear strain rate and initial mean particle contact angle were used, as shown in Eq. (10).

$$\frac{dN_f}{dt^*} \cong -\frac{\lambda \cdot \dot{\gamma}_0}{A_{cm} \cdot \cos\theta_{cm0}} \cdot N_f \quad (10)$$

where $\dot{\gamma}_0$ is initial shear strain rate under a shear force, and θ_{cm0} is initial mean cementitious particle contact angle in the beginning of applying a shear force.

By substituting Eq. (4) into Eq. (10), the change in the number of flocculated particles with shearing time t^* was expressed by Eq. (11).

$$\frac{dN_f}{dt^*} \cong -\frac{\lambda \cdot \dot{\gamma}_0}{A_m \cos\theta_{cm0}} \cdot N \cdot \left[1 - \beta \cdot (t^* + t_0) - \frac{3\eta \cdot N_{d0}/N}{8kT \cdot N_{d0} \cdot (t^* + t_0) + 3\eta} \right] \quad (11)$$

where t_0 is rest time from concrete mixing to re-agitation, t_0 plus t^* is equal to the elapsed time (t) after mixing.

By integrating the two sides of Eq. (11) with respect to t^* , the number (N_{fa}) of residual flocculated particles at any shearing time t^* in agitated state was obtained, as shown in Eq. (12).

$$N_{fa} \cong -\frac{\lambda \cdot \dot{\gamma}_0}{A_m \cos\theta_{cm0}} \cdot \left[N \cdot t^* - \beta \cdot t_0 \cdot t^* - \frac{\beta(t^*)^2}{2} - \frac{3\eta N_{d0}/N}{8kT N_{d0}} \cdot \ln(8kT N_{d0} \cdot t^* + 3\eta + 8kT N_{d0} \cdot t_0) \right] + N \cdot \left(1 - \beta \cdot t_0 - \frac{3\eta N_{d0}/N}{8kT N_{d0} \cdot t_0 + 3\eta} \right) - \frac{\lambda \cdot \dot{\gamma}_0}{A_m \cos\theta_{cm0}} \cdot \frac{3\eta N_{d0}/N}{8kT} \cdot \ln(8kT N_{d0} \cdot t_0 + 3\eta) \quad (12)$$

Therefore, the number (N_{ha}) of chemically bonded cementitious particles and the number (N_{da}) of dispersed cementitious particles in agitated state are expressed by

$$N_{ha} = N \cdot \frac{t_0 + t^*}{t_i} \cdot \exp\left[\frac{E}{R} \left(\frac{1}{293} - \frac{1}{273 + T} \right)\right] \quad (13)$$

$$N_{da} = N - N_{ha} - N_{fa} \quad (14)$$

In present DEM, fresh concrete is represented by discrete particles, and every discrete particle has the same components that are cementitious particles, aggregate particles and water. For convenience, we supposed that the numbers of three types of discrete particle are proportional to those of three types of cementitious particle. The proportional constant is a ratio of total discrete particles of fresh concrete to cementitious particles in quantity.

$$N_{fa}^d = \frac{N^*}{N} \cdot N_{fa}, N_{ha}^d = \frac{N^*}{N} \cdot N_{ha}, N_{da}^d = \frac{N^*}{N} \cdot N_{da} \quad (15)$$

where N_{fa}^d , N_{ha}^d , N_{da}^d are numbers of flocculated, clumped, and dispersed discrete particles, respectively, and N^* is number of total discrete particles

2.3. Normal and shear stiffness of the parallel bond model

In general DEM, the normal and shear stiffnesses k_n , k_s of the parallel bond model are dealt with two constants. But in case of fresh concrete, the number of flocculated cementitious particles varies with standing time or agitation's intensity and time. With the increase of the flocculated cementitious particles, the contacts of the discrete particles become strong on average, thus the movement of discrete particles becomes hard for a given external force. That is to say, the contacts become uneasy to be broken. The stiffnesses k_n , k_s should not be two constants, varying with the number of flocculated particles. For describing the time-dependence of fresh concrete, we treated the increase of flocculated cementitious particles with the growth of contact intensity of discrete particles, assuming that the normal and shear stiffness k_n , k_s increase linearly with the number of flocculated cementitious particles in this study. The normal and shear stiffness k_{nt} , k_{st} at time t ($=t_0 + t^*$) of the parallel bond model in agitated state later after rest are expressed by Eqs. (16) and (17).

$$k_{nt} = \frac{N_{fa}}{N} \cdot \Delta k_n + k_{n0} \quad (16)$$

$$k_{st} = \frac{N_{fa}}{N} \cdot \Delta k_s + k_{s0} \quad (17)$$

where k_{nt} , k_{st} are normal and shear stiffness of flocculated discrete particle at time t , respectively, k_{n0} , k_{s0} are normal and shear stiffnesses in the beginning (rest time $t_0 = 0$), respectively, and Δk_n , Δk_s are proportional constants of the increases in normal and shear stiffness with flocculated cementitious particles, respectively.

Because the normal and shear stiffness k_{nt} , k_{st} shown in Eqs. (16) and (17) reflect the effects of rest and agitation simultaneously, the numerical analysis using the present DEM, of which the parallel bond model adopts the stiffnesses k_{nt} , k_{st} , is able to treat the thixotropic phenomenon of fresh concrete. Also, the effect of cement hydration is considered by introducing the clumped particles in this new DEM. Hence, this new DEM model can also treat the time-dependence of fluidity of fresh concrete, resulting from cement hydration. Here, we call briefly this new DEM as rest & shearing time-dependent DEM.

3. Verification of rest & shearing time-dependent DEM

The rest & shearing time-dependent DEM is proposed for fresh concrete, but it is also applied to fresh mortar, because fresh mortar has viscous, granular, and time-dependent characteristics like fresh concrete though its aggregate's maximum size is small.

Table 1
Mean flow table values of three mortars.

Series	No. 1	No. 2	No. 3
Right after mixing (mm)	210	253	265
After 10 min rest (mm)	135	182	205

Therefore, it is allowed to use fresh mortar to verify the validity of present DEM. Besides this, there are other reasons for using fresh concrete in the verification experiments, as stated in the following.

Since the thixotropy of fresh cementitious materials is mainly caused by physical flocculation of cement, the use of coarse aggregate not only lowers the precisions of rheological experiment, but also would cause the thixotropic characteristic so obscure that is

hard to experimentally observe. The precipitation of coarse aggregate particles in standing state results in the instability of fresh concrete's property, which also obstructs the experimental observation of thixotropic phenomenon. Moreover, because the volume of fresh concrete sample needed in rheological test is larger than fresh mortar, the numerical analysis of concrete has to use a lot of discrete particles and wall particles, thus long computation time or high performance computer is necessary.

3.1. Flow table test and rheological test

Three series of mortars were used in the flow table test and the rheological test. Series No. 1 used only ordinary Portland cement as

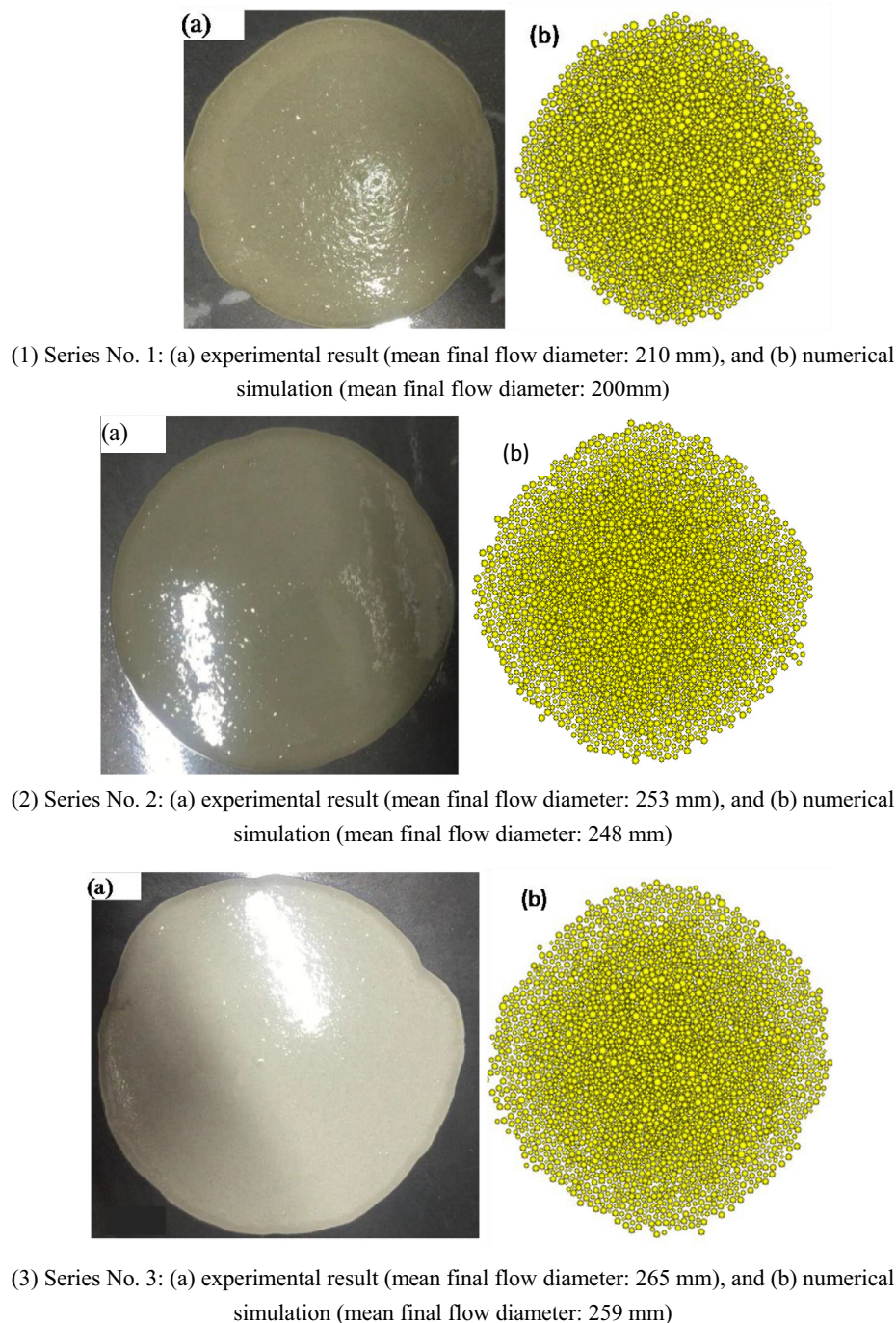


Fig. 2. Experimental and numerical results of the flow table test right after mixing.

binder without the addition of any mineral admixture, but in Series No. 2, JIS (Japanese Industrial Standards) Type II fly ash (FA) replaced 20% of ordinary Portland cement, and in Series No. 3, ground granulated blast furnace slag (BFS) of JIS 8000 Class was used in place of 50% of ordinary Portland cement. The specific surface areas of the FA and the BFS were 4040 and 7980 cm²/g, respectively. Details about mix proportions of the mortars, used fine aggregate and chemical admixtures, the compositions of ordinary Portland cement, FA and BFS, and mixing method of mortar samples can be found in Ref. [14]. Right after mixing, part of mortar sample was used to do the flow table test for calibrating the input parameters of rest & shearing time-dependent DEM, the remains were used to do the rheological test using a B-type rheometer.

The cone used in the flow table test has upper diameter of 40 mm, lower diameter of 90 mm, and 75 mm height. The flow table test was conducted three times for every mortar, and final diameters were measured. Mean final flow diameter of three times tests was calculated for each mortar. The flow table test was done right after mixing and after 10 min rest ($t_0 = 10$ min). Rest time t_0 was the elapsed time from the time point when the mortar sample was completely mixed. Experimental results of the flow table test are shown in Table 1. Examples of final flow shape of the flow table test right after mixing and after 10 min rest are shown respectively in Figs. 2 and 3 (1)–(3) (a) for the three mortars.

The B-type viscometer used in the rheological test is shown in Fig. 4(a). The #3 rotor was used as shown in Fig. 4(b). The geometry

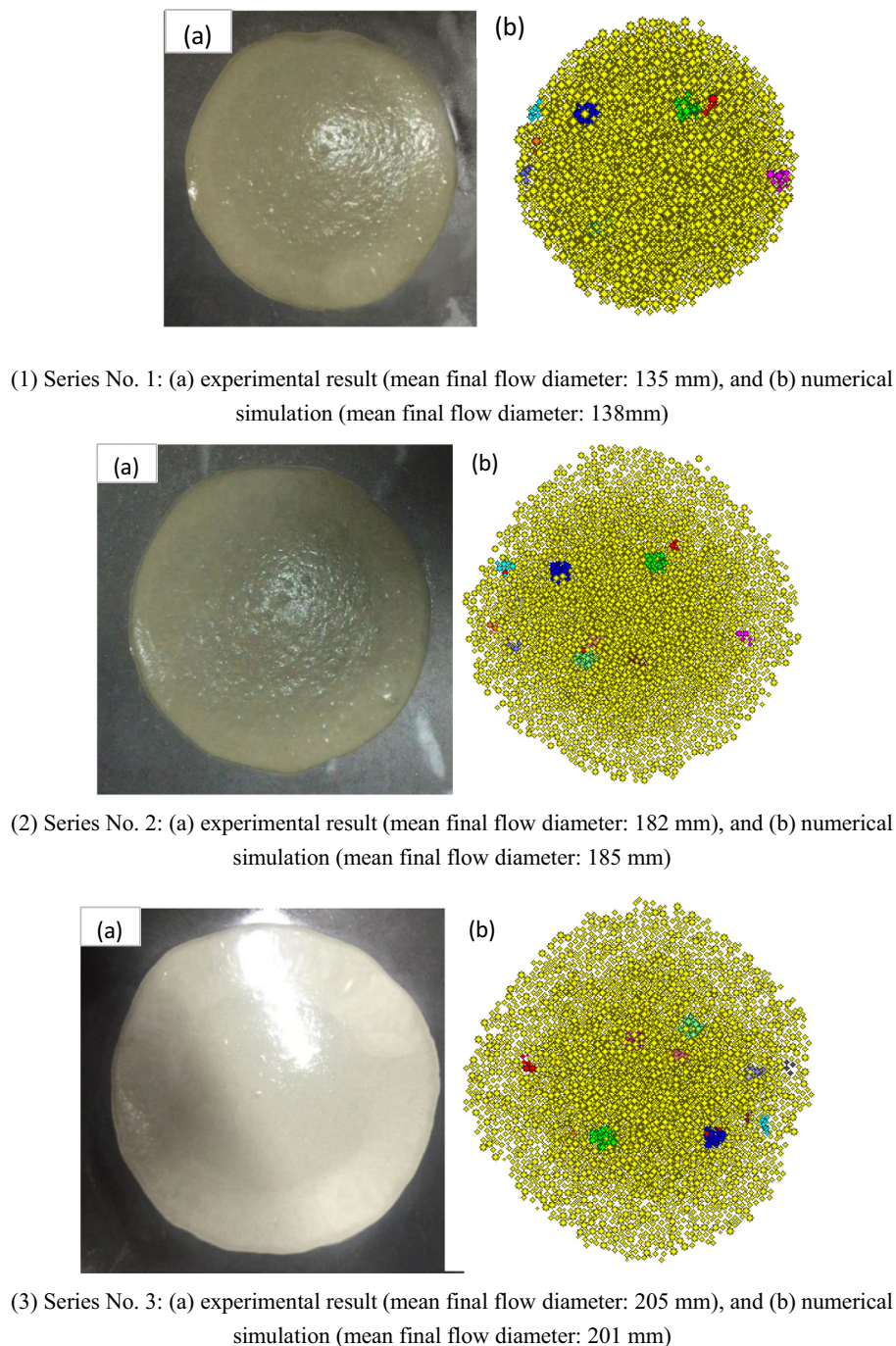


Fig. 3. Experimental and numerical results of the flow table test after 10 min rest.

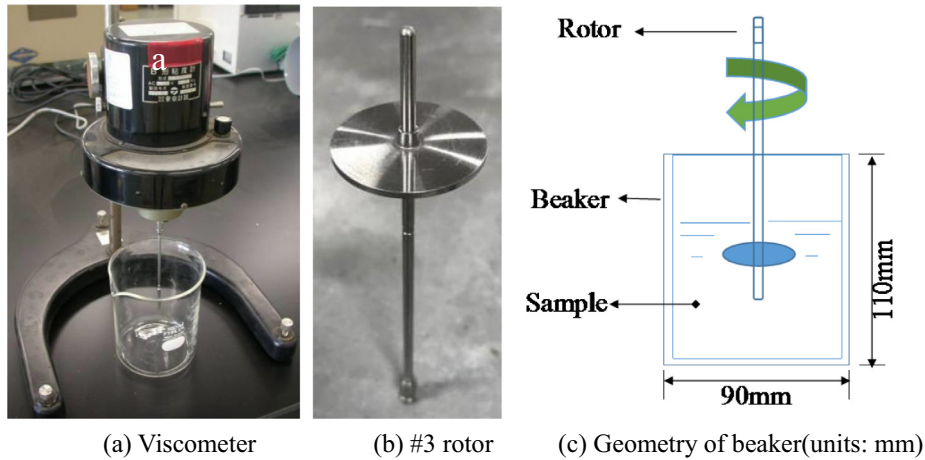


Fig. 4. Viscometer, #3 rotor, and beaker used for the rheological test.

of sample beaker is shown in Fig. 4(c). The viscometer is operated by rotational speed growth control method. The torque that acts on the rotor, corresponding to a rotational speed, is calculated by

$$T = k_b \theta \tag{18}$$

where T is torque (mPa·s), k_b is torsion constant (N·m), θ is rotational angle of pointer.

Right after mixing, the rheological test was done for the first time. The rotational angles of pointer and rotating times at the rotational speeds of 0.5, 1, 2.5, 5, and 10 rpm were recorded, respectively. At 5 min interval of rest later after the first measurement, the rheological test was conducted repeatedly for Series No. 1 and Series No. 2. However, because Series No. 3 had relatively higher fluidity than other two series, the rest time interval was set to be 10 min. The measuring results of hysteresis loop of torque-rotational speed relation are shown in Fig. 5.

3.2. Calibration of the input parameters of DEM simulation

The flow table test is mostly used to evaluate the flow ability of fresh mortar. In this study, the input parameters of DEM simulation were calibrated through simulating the flow table test. That is to say, all the input parameters were iteratively adjusted until the numerical results of the flow table test agreed with the experimental results of mean flow diameter. The numerical simulation results of the flow table test conducted right after mixing and after 10 min rest were shown in Figs. 2 and 3 (1)–(3) (b), respectively. Right after mixing there was no clumped particle. However, after 10 min rest, several clumped particles were found, marked in several kinds of color except yellow as shown in Fig. 3 (1)–(b) (b).

In the DEM simulation, if the size distribution of discrete particles was set to be the same to actual particles of mortar, the numerical calculation becomes complicated and time-consuming. Hence, the diameters of discrete particles were in a range of 1.5–3.0 mm here. 4378 discrete particles were used in the DEM simulation of the flow table test. The porosity of three fresh mortars was 0.22. Details about the determination of the porosity can be found in Ref. [13].

The inter-frictional resistance of mortar depends on its subjected vertical pressure that is usually resulted from its self-gravity. Because there are voids in fresh mortar, total volume of discrete particles becomes less than that of mortar sample. That is to say, if using actual specific gravity of mortar in the calculation, the vertical pressure acting on discrete particles is smaller than the actual value. For making the pressure applied to discrete particles equal to the actual value, the specific gravity of discrete particle

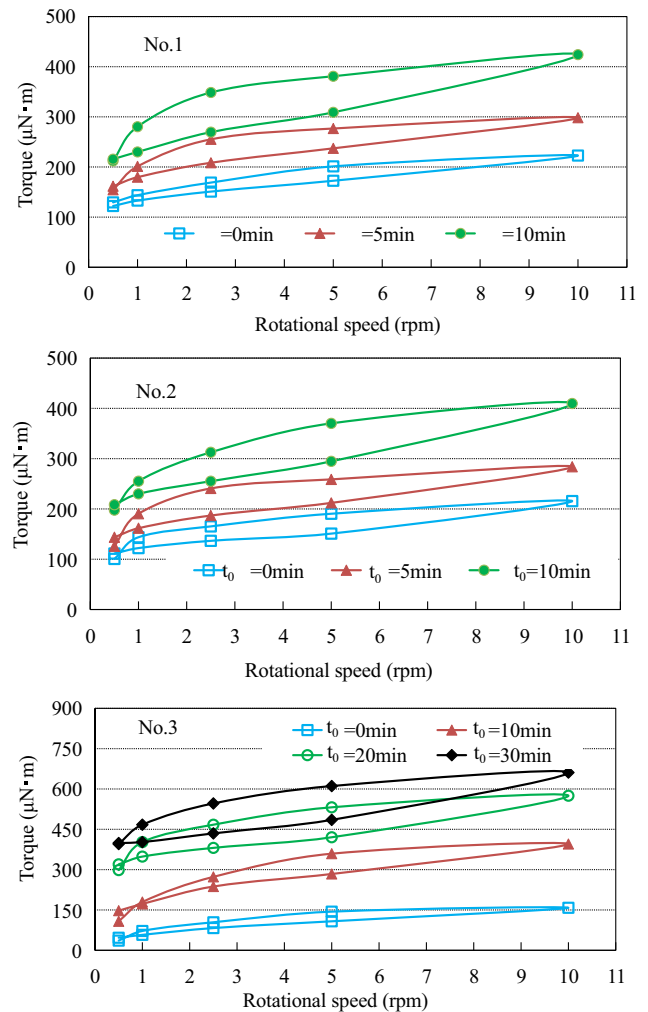


Fig. 5. Experimental results of torque – rotational speed relationship.

was increased. Discrete particle's densities of three series of mortar were set to be 2897 kg/m³ (No. 1), 2628 kg/m³ (No. 2), and 2743 kg/m³ (No. 3), respectively.

The parameters in Eqs. (1)–(2) and Eq. (12) were set, as shown in Table 2, on basis of raw materials used and mix proportions of the mortars. Based on the simulation of the flow table test as

Table 2
The input parameters for the mortar mixtures.

Series	E (J/mol)	t_i (min)	A_{cm} (mm, $\times 10^{-12}$)	Δt (min)	T ($^{\circ}\text{C}$)	P_{C3A} (%)	P_{C4AF} (%)	B (m^2/kg)	N	η (Pa·s)	λ
No. 1	44,977	360	8.0	5	20	9	9	356	$5\text{E}+17$	0.001	$5\text{E}-16$
No. 2	36,593	420	7.5								
No. 3	53,972	480	10.0	10							

Table 3
The parameters for the mortar's discrete particles and wall elements.

Element of DEM	Fresh mortar's series	k_n^p, k_n^w (N/m^3)	k_s^p, k_s^w (N/m^3)	f^p, f^w	r (mm)
Discrete particle	No. 1	1200	200	0.2	1.5–3.0
	No. 2	50	20		
	No. 3	35	15		
Wall	No. 1, No. 2, No. 3	$2 \times \text{E} + 06$	$2 \times \text{E} + 06$	0.4	–

[Notes] r : particle radius, f^p, f^w : frictional coefficient of discrete particle, and wall element, respectively.

Table 4
The parameters of the parallel bond model and the viscous damping model.

Series	k_{n0} (N/m^3)	k_{s0} (N/m^3)	Δk_n (N/m^3)	Δk_s (N/m^3)	σ_c (N/m^2)	τ_c (N/m^2)	l	C_n	C_s
No. 1	1000	400	3966	1305	550	22	0.5	0.3	0.1
No. 2	90	50	415	83					
No. 3	55	20	310	52					

shown in Figs. 3 and 4, the parameters for the discrete particles and wall elements were obtained, as shown in Table 3, and the parameters of the viscous damping model and the parallel bond model are gotten, as presented in Table 4.

3.3. Comparison between experimental and numerical results of hysteresis loop

As stated above, we filled mortar sample into a beaker right after mixing. Next, we let the rotor rotate at a speed of 0.5 rpm, and then raised rotational speed to 1 rpm, 2.5 rpm, 5 rpm, and 10 rpm, further dropped the rotational speed. At every speed level, the stable angle value (θ) and the rotating time, when the angle pointer reached to the stable value, were recorded. The torque corresponding to each rotational speed was calculated by substituting the angle into Eq. (18). The test results of hysteresis loop of torque – rotational speed relationship are shown in Fig. 5.

The numerical calculations were carried out for the viscometer test using the proposed DEM. Each of mortar sample, filled into the beaker for the viscometer test, was modeled by 5903 discrete particles (orange-colored), and the rotor was represented by 32 wall elements (dark blue-colored), as shown in Fig. 6.

The number (N_{ha}) of hydrated cementitious particles at time t ($=t^* + t_0$) was calculated by using Eq. (13), and the number (N_{fa}) of the residual flocculated cementitious particles was obtained by Eq. (12). Accordingly, the number (N_{da}) of the dispersed cementitious particles was gotten by subtracting the N_h and the N_{fa} from the total number (N) of cementitious particles, as shown in Eq. (14). Then, the numbers at time t , of three types of discrete particles (clumped, flocculated and dispersed), were gotten by multiplying N_h, N_{fa}, N_d by a coefficient ($=5903/N$), respectively, according Eq. (15). The interactions between dispersed discrete particles, flocculated discrete particles, and clumped discrete particles follow the models shown in Fig. 1(a)–(c), respectively. The normal and shear stiffness (k_{nt}, k_{st}) at time t of the parallel bond model was calculated on basis of the N_{fa} by using Eqs. (16) and (17).

The interaction between fresh mortar and rotor was regarded as the interaction between discrete particles and wall elements, following the interaction model shown in Fig. 1(a). The rotor rotation

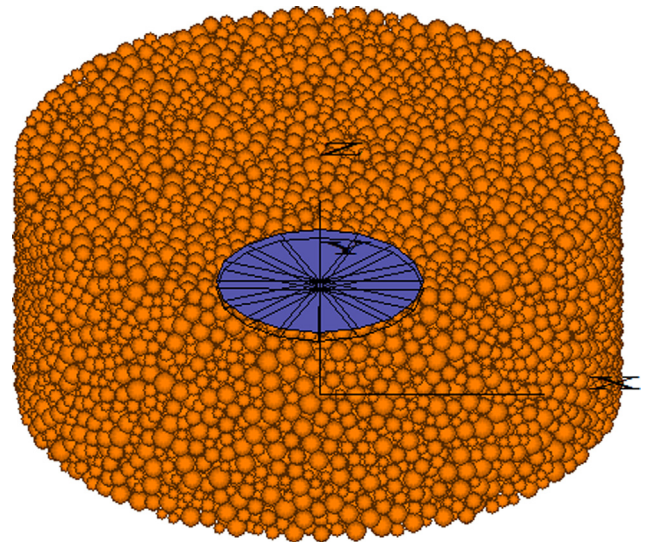


Fig. 6. Simulation of viscometer test immediately after mixed.

at a series of designated speeds was represented by simultaneous rotation of the 32 wall elements under the translational and rotational velocities. At every calculating step, the distances between discrete particles and wall elements were checked to determine which discrete particle got in contact with any of the wall elements. The discrete particles, contacting with the wall elements, were acted by one or more wall elements. The action was calculated according to the force-displacement law (Esq. (2) and (3) in our past report [14]). The displacement means relative motion between discrete particle and wall element, including relatively moving distance and rotational angle. In the instant when the wall elements start to rotate, there is about to cause a relative motion because the discrete particles are at rest in the beginning. However, the relative motion doesn't really occur because the interaction makes the discrete particles rotate together with the rotor.

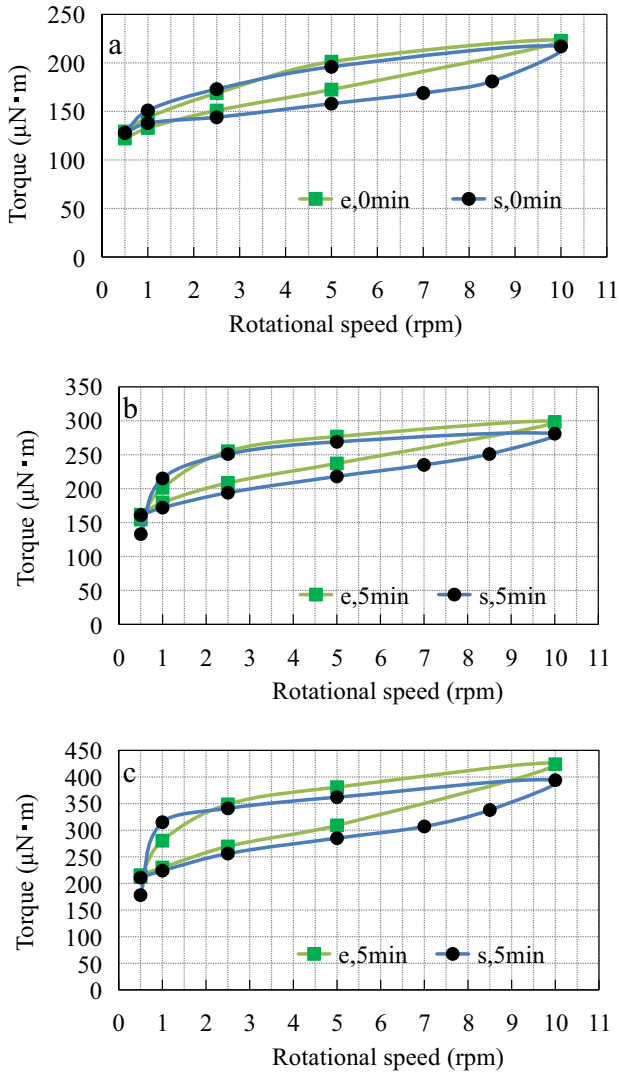


Fig. 7. Comparison between experimental and numerical results of torque – rotational speed relationship (Series No. 1), (Rest time:(a) 0 min, (b) 5 min, and (c) 10 min).

Figs. 7–9 show the numerical results together with the experimental results, In these figures, and “e” and “s” represent experimental and numerical result, respectively. As shown in Figs. 7–9, at the rotational speed of 0.5 rpm, all the calculating torques are slightly greater than the experimental values, but at 5 rpm and 10 rpm of rotational speed, the calculating torques are slightly smaller than the measuring values. Maybe this is because air bubbles in the mortar lowered the experimental values in the early stage. With the rotation of the rotor, the air bubbles surrounding the rotor got out, and measuring torque thus increased. However, the numerical results of hysteresis loop are very similar to the experimental results. And the numerical results indicate that the torque increases with the prolongation of rest period even for a certain rotational speed as the experimental results.

For comparing quantitatively the experimental and numerical results of hysteresis loop, we measured the areas of the hysteresis loops. First, the areas (A_u, A_d) between the horizontal axis and the up curve, and the down curve were measured respectively by summing up the number of grids. One grid has a size of $50 \mu\text{Nm} \times 0.5 \text{rpm}$ ($=25$) as shown in Figs. 7–9. For fragmented grids, their areas were roughly estimated according to the proportion of the part under the curve to a grid. The area of hysteresis loop is a difference between A_u and A_d .

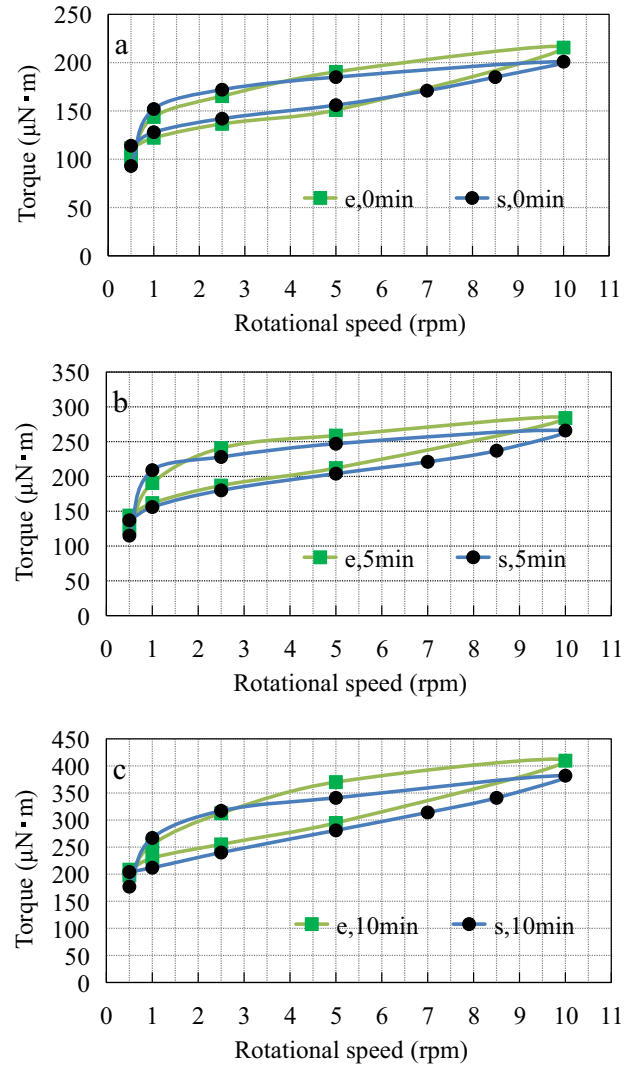


Fig. 8. Comparison between experimental and numerical results of torque – rotational speed relationship (Series No. 2), (Rest time: (a) 0 min, (b) 5 min, and (c) 10 min).

The areas of the hysteresis loops were shown in Fig. 10 for different mortars and different rest times. And the errors of the numerical results (s) relative to the experimental results (e) are also presented in Fig. 10. The error is equal to $(s-e)/e \times 100\%$. Fig. 10 indicates that the numerical results are close to the experimental results, and the errors are within $\pm 20\%$. In case of using mineral admixture (FA or BFS), the errors are very small except 0 min of rest time. Also, the area of hysteresis loop increases with the increase of rest time for a certain mortar mixture, and it is in an order of No. 1, No. 2, and No. 3 for the same rest time (10 min). That is to say, the mortar that has been kept a long time of rest shows more remarkable thixotropic characteristic, and the mortar without using mineral admixture is more thixotropic, compared to the mixtures using FA or BFS to replace part of ordinary Portland cement.

4. Conclusions

The time-dependent behaviors of fresh concrete are generally considered to result from the reversible dispersion-flocculation of cement particles and the irreversible particle bonds caused by the hydrates of cement. In this study, in order to predict the

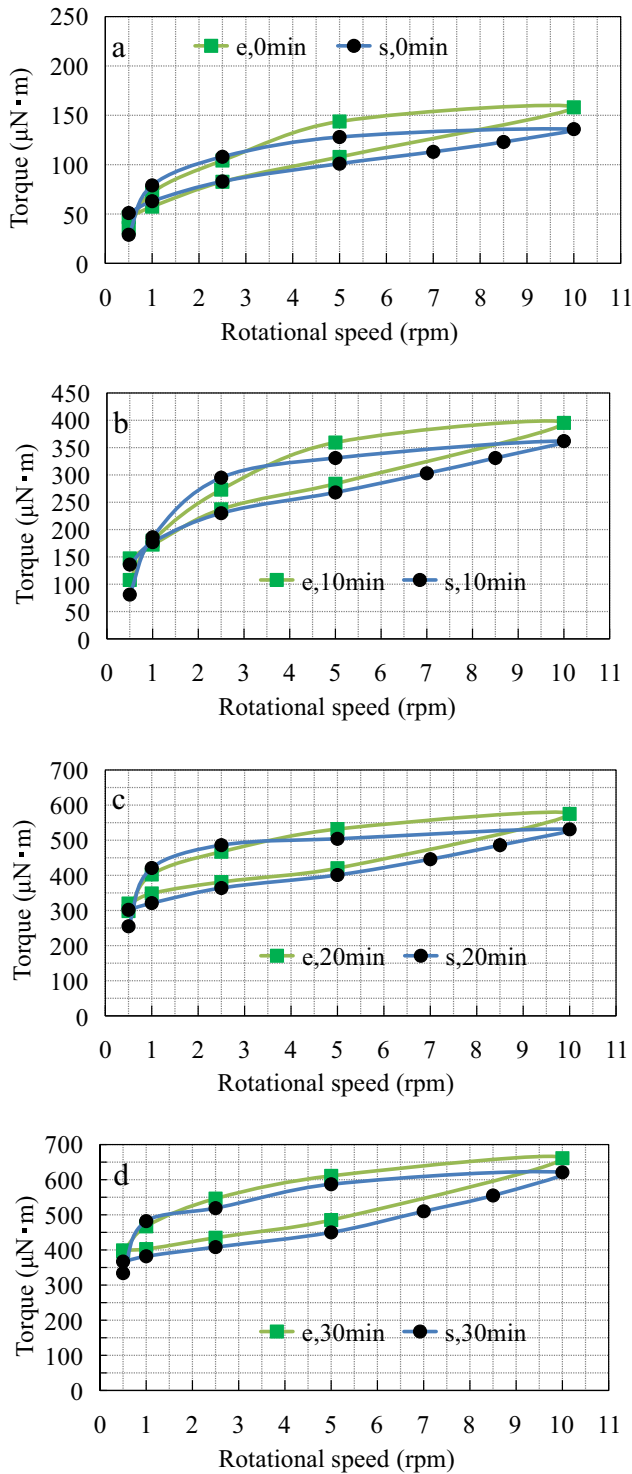


Fig. 9. Comparison between experimental and numerical results of torque – rotational speed relationship (Series No. 3), (Rest time:(a) 0 min, (b) 10 min, (c) 20 min, and (d) 30 min).

thixotropic behavior of fresh concrete, rest & shearing time-dependent DEM (td-DEM) was further developed on the basis of the rest time-dependent DEM [14]. Fresh concrete was represented by imaginary discrete particles. Viscous damping model was used to describe the interactions between dispersed discrete particles. The parallel bond model was employed to describe the interactions and contact failure conditions of physically flocculated particles, and the clumped particles were introduced to represent the particle assembly bonded chemically by the hydrates of cement.

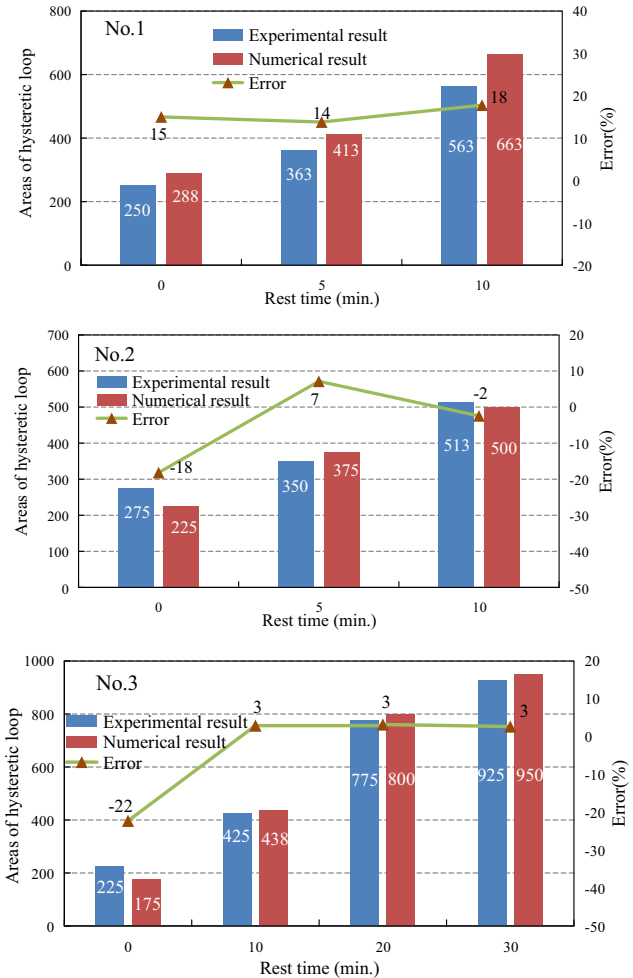


Fig. 10. Comparison of the numerical and experimental results of hysteresis loop's area for different mortars and rest times.

The change of the number of flocculated particles with shearing time in an agitated state was investigated theoretically, as shown in Eq. (12). Then time-dependent normal and shear stiffnesses of the parallel bond model in an agitated state were then proposed, as shown in Eqs. (16) and (17).

For verifying the td-DEM, the simulations of the B-type viscometer test for three mortar mixtures were conducted. The input parameters of the td-DEM were calibrated by the flow table test. Based on the obtained input parameters, the hysteresis loops of torque-rotational speed relationship were simulated for different mortar mixture and different rest times. The numerical results of hysteresis loop's area and shape were very close to the experimental results, and it is concluded that the longer the rest time, or the greater the cement content, the more thixotropic the fresh cementitious materials. The td-DEM can properly predict the thixotropic behaviors of fresh concrete with or without mineral admixture.

Conflict of interest

The authors declared that they have no conflicts of interest to this work.

References

[1] N. Roussel, A theoretical frame to study stability of fresh concrete, *Mater. Struct.* 39 (1) (2006) 81–91.

- [2] T.T. Le, S.A. Austin, S. Lim, et al., Mix design and fresh properties for high-performance printing concrete, *Mater. Struct.* 45 (8) (2012) 1221–1232.
- [3] N. Roussel, F. Cussigh, Distinct-layer casting of SCC: the mechanical consequences of thixotropy, *Cem. Concr. Res.* 38 (5) (2008) 624–632.
- [4] T. Lecompte, A. Perrot, Non-linear modeling of yield stress increase due to SCC structural build-up at rest, *Cem. Concr. Res.* 92 (2017) 92–97.
- [5] Z. Li, Bleeding model of fresh concrete in still state, *J. Struct. Constr. Eng. Arch. Inst. Jpn.* 77 (679) (2012) 1357–1366.
- [6] H.A. Barnes, Thixotropy—a review, *J. Nonnewton. Fluid Mech.* 70 (1–2) (1997) 1–33.
- [7] G.H. Tattersall, P. Banfill, *The rheology of fresh concrete*, Pitman London (1983).
- [8] Z. Li, T. Ohkubo, Y. Tanigawa, Theoretical analysis of time-dependence and thixotropy of fluidity for high fluidity concrete, *J. Mater. Civ. Eng.* 16 (3) (2004) 247–256.
- [9] P. Coussot, Q. Nguyen, H. Huynh, et al., Viscosity bifurcation in thixotropic, yielding fluids, *J. Rheol.* 46 (3) (2002) 573–589.
- [10] N. Roussel, Steady and transient flow behaviour of fresh cement pastes, *Cem. Concr. Res.* 35 (9) (2005) 1656–1664.
- [11] N. Roussel, A thixotropy model for fresh fluid concretes: theory, validation and applications, *Cem. Concr. Res.* 36 (10) (2006) 1797–1806.
- [12] P. Coussot, Q.D. Nguyen, H. Huynh, et al., Avalanche behavior in yield stress fluids, *Phys. Rev. Lett.* 88 (17) (2002) 175501.
- [13] Z. Li, G. Cao, Y. Tan, Prediction of time-dependent flow behaviors of fresh concrete, *Constr. Build. Mater.* 125 (2016) 510–519.
- [14] G. Cao, Z. Li, K. Guo, Analytical study on the change of fluidity of fresh concrete containing mineral admixture with rest time, *J. Adv. Concr. Technol.* 15 (11) (2017) 713–723.
- [15] R. Pieralisi, S. Cavalaro, A. Aguado, Discrete element modelling of the fresh state behavior of pervious concrete, *Cem. Concr. Res.* 90 (2016) 6–18.
- [16] Y. Tan, R. Deng, Y. Feng, et al., Numerical study of concrete mixing transport process and mixing mechanism of truck mixer, *Eng. Comput.* 32 (4) (2015) 1041–1065.
- [17] Z. Li, T. Ohkubo, Y. Tanigawa, Flow performance of high-fluidity concrete, *J. Mater. Civ. Eng.* 16 (6) (2004) 588–596.